

Midrapidity  $\phi$  production in Au+Au collisions at  $\sqrt{s_{NN}}=130$  GeV

C. Adler,<sup>11</sup> Z. Ahammed,<sup>23</sup> C. Allgower,<sup>12</sup> J. Amonett,<sup>14</sup> B. D. Anderson,<sup>14</sup> M. Anderson,<sup>5</sup> G. S. Averichev,<sup>9</sup> J. Balewski,<sup>12</sup> O. Barannikova,<sup>9,23</sup> L. S. Barnby,<sup>14</sup> J. Baudot,<sup>13</sup> S. Bekele,<sup>20</sup> V. V. Belaga,<sup>9</sup> R. Bellwied,<sup>30</sup> J. Berger,<sup>11</sup> H. Bichsel,<sup>29</sup> L. C. Bland,<sup>12</sup> C. O. Blyth,<sup>3</sup> B. E. Bonner,<sup>24</sup> A. Boucham,<sup>26</sup> A. Brandin,<sup>18</sup> R. V. Cadman,<sup>1</sup> H. Caines,<sup>20</sup> M. Calderón de la Barca Sánchez,<sup>31</sup> A. Cardenas,<sup>23</sup> J. Carroll,<sup>15</sup> J. Castillo,<sup>26</sup> M. Castro,<sup>30</sup> D. Cebra,<sup>5</sup> S. Chattopadhyay,<sup>30</sup> M. L. Chen,<sup>2</sup> Y. Chen,<sup>6</sup> S. P. Chernenko,<sup>9</sup> M. Cherney,<sup>8</sup> A. Chikanian,<sup>31</sup> B. Choi,<sup>27</sup> W. Christie,<sup>2</sup> J. P. Coffin,<sup>13</sup> T. M. Cormier,<sup>30</sup> J. G. Cramer,<sup>29</sup> H. J. Crawford,<sup>4</sup> M. DeMello,<sup>24</sup> W. S. Deng,<sup>14</sup> A. A. Derevschikov,<sup>22</sup> L. Didenko,<sup>2</sup> J. E. Draper,<sup>5</sup> V. B. Dunin,<sup>9</sup> J. C. Dunlop,<sup>31</sup> V. Eckardt,<sup>16</sup> L. G. Efimov,<sup>9</sup> V. Emelianov,<sup>18</sup> J. Engelage,<sup>4</sup> G. Eppley,<sup>24</sup> B. Erasmus,<sup>26</sup> P. Fachini,<sup>25</sup> V. Faine,<sup>2</sup> E. Finch,<sup>31</sup> Y. Fisyak,<sup>2</sup> D. Flierl,<sup>11</sup> K. J. Foley,<sup>2</sup> J. Fu,<sup>15</sup> N. Gagunashvili,<sup>9</sup> J. Gans,<sup>31</sup> L. Gaudichet,<sup>26</sup> M. Germain,<sup>13</sup> F. Geurts,<sup>24</sup> V. Ghazikhanian,<sup>6</sup> J. Grabski,<sup>28</sup> O. Grachov,<sup>30</sup> D. Greiner,<sup>15</sup> V. Grigoriev,<sup>18</sup> M. Guedon,<sup>13</sup> E. Gushin,<sup>18</sup> T. J. Hallman,<sup>2</sup> D. Hardtke,<sup>15</sup> J. W. Harris,<sup>31</sup> M. Heffner,<sup>5</sup> S. Heppelmann,<sup>21</sup> T. Herston,<sup>23</sup> B. Hippolyte,<sup>13</sup> A. Hirsch,<sup>23</sup> E. Hjort,<sup>15</sup> G. W. Hoffmann,<sup>27</sup> M. Horsley,<sup>31</sup> H. Z. Huang,<sup>6</sup> T. J. Humanic,<sup>20</sup> H. Hümmeler,<sup>16</sup> G. Igo,<sup>6</sup> A. Ishihara,<sup>27</sup> Yu. I. Ivanshin,<sup>10</sup> P. Jacobs,<sup>15</sup> W. W. Jacobs,<sup>12</sup> M. Janik,<sup>28</sup> I. Johnson,<sup>15</sup> P. G. Jones,<sup>3</sup> E. Judd,<sup>4</sup> M. Kaneta,<sup>15</sup> M. Kaplan,<sup>7</sup> D. Keane,<sup>14</sup> A. Kisiel,<sup>28</sup> J. Klay,<sup>5</sup> S. R. Klein,<sup>15</sup> A. Klyachko,<sup>12</sup> A. S. Konstantinov,<sup>22</sup> L. Kotchenda,<sup>18</sup> A. D. Kovalenko,<sup>9</sup> M. Kramer,<sup>19</sup> P. Kravtsov,<sup>18</sup> K. Krueger,<sup>1</sup> C. Kuhn,<sup>13</sup> A. I. Kulikov,<sup>9</sup> G. J. Kunde,<sup>31</sup> C. L. Kunz,<sup>7</sup> R. Kh. Kutuev,<sup>10</sup> A. A. Kuznetsov,<sup>9</sup> L. Lakehal-Ayat,<sup>26</sup> J. Lamas-Valverde,<sup>24</sup> M. A. C. Lamont,<sup>3</sup> J. M. Landgraf,<sup>2</sup> S. Lange,<sup>11</sup> C. P. Lansdell,<sup>27</sup> B. Lasiuk,<sup>31</sup> F. Laue,<sup>2</sup> A. Lebedev,<sup>2</sup> T. LeCompte,<sup>1</sup> R. Lednický,<sup>9</sup> V. M. Leontiev,<sup>22</sup> M. J. LeVine,<sup>2</sup> Q. Li,<sup>30</sup> Q. Li,<sup>15</sup> S. J. Lindenbaum,<sup>19</sup> M. A. Lisa,<sup>20</sup> T. Ljubicic,<sup>2</sup> W. J. Llope,<sup>24</sup> G. LoCurto,<sup>16</sup> H. Long,<sup>6</sup> R. S. Longacre,<sup>2</sup> M. Lopez-Noriega,<sup>20</sup> W. A. Love,<sup>2</sup> D. Lynn,<sup>2</sup> R. Majka,<sup>31</sup> S. Margetis,<sup>14</sup> L. Martin,<sup>26</sup> J. Marx,<sup>15</sup> H. S. Matis,<sup>15</sup> Yu. A. Matulenko,<sup>22</sup> T. S. McShane,<sup>8</sup> F. Meissner,<sup>15</sup> Yu. Melnick,<sup>22</sup> A. Meschanin,<sup>22</sup> M. Messer,<sup>2</sup> M. L. Miller,<sup>31</sup> Z. Milosevich,<sup>7</sup> N. G. Minaev,<sup>22</sup> J. Mitchell,<sup>24</sup> V. A. Moiseenko,<sup>10</sup> D. Moltz,<sup>15</sup> C. F. Moore,<sup>27</sup> V. Morozov,<sup>15</sup> M. M. de Moura,<sup>30</sup> M. G. Munhoz,<sup>25</sup> G. S. Mutchler,<sup>24</sup> J. M. Nelson,<sup>3</sup> P. Nevski,<sup>2</sup> V. A. Nikitin,<sup>10</sup> L. V. Nogach,<sup>22</sup> B. Norman,<sup>14</sup> S. B. Nurushev,<sup>22</sup> G. Odyniec,<sup>15</sup> A. Ogawa,<sup>21</sup> V. Okorokov,<sup>18</sup> M. Oldenburg,<sup>16</sup> D. Olson,<sup>15</sup> G. Paic,<sup>20</sup> S. U. Pandey,<sup>30</sup> Y. Panebratsev,<sup>9</sup> S. Y. Panitkin,<sup>2</sup> A. I. Pavlinov,<sup>30</sup> T. Pawlak,<sup>28</sup> V. Perevoztchikov,<sup>2</sup> W. Peryt,<sup>28</sup> V. A. Petrov,<sup>10</sup> E. Platner,<sup>24</sup> J. Pluta,<sup>28</sup> N. Porile,<sup>23</sup> J. Porter,<sup>2</sup> A. M. Poskanzer,<sup>15</sup> E. Potrebenikova,<sup>9</sup> D. Prindle,<sup>29</sup> C. Pruneau,<sup>30</sup> S. Radomski,<sup>28</sup> G. Rai,<sup>15</sup> O. Ravel,<sup>26</sup> R. L. Ray,<sup>27</sup> S. V. Razin,<sup>9,12</sup> D. Reichhold,<sup>8</sup> J. G. Reid,<sup>29</sup> F. Retiere,<sup>15</sup> A. Ridiger,<sup>18</sup> H. G. Ritter,<sup>15</sup> J. B. Roberts,<sup>24</sup> O. V. Rogachevski,<sup>9</sup> J. L. Romero,<sup>5</sup> C. Roy,<sup>26</sup> D. Russ,<sup>7</sup> V. Rykov,<sup>30</sup> I. Sakrejda,<sup>15</sup> J. Sandweiss,<sup>31</sup> A. C. Saulys,<sup>2</sup> I. Savin,<sup>10</sup> J. Schambach,<sup>27</sup> R. P. Scharenberg,<sup>23</sup> N. Schmitz,<sup>16</sup> L. S. Schroeder,<sup>15</sup> A. Schüttauf,<sup>16</sup> K. Schweda,<sup>15</sup> J. Seger,<sup>8</sup> D. Seliverstov,<sup>18</sup> P. Seyboth,<sup>16</sup> E. Shahaliev,<sup>9</sup> K. E. Shestermanov,<sup>22</sup> S. S. Shimanskii,<sup>9</sup> V. S. Shvetcov,<sup>10</sup> G. Skoro,<sup>9</sup> N. Smirnov,<sup>31</sup> R. Snellings,<sup>15</sup> J. Sowinski,<sup>12</sup> H. M. Spinka,<sup>1</sup> B. Srivastava,<sup>23</sup> E. J. Stephenson,<sup>12</sup> R. Stock,<sup>11</sup> A. Stolpovsky,<sup>30</sup> M. Strikhanov,<sup>18</sup> B. Stringfellow,<sup>23</sup> C. Struck,<sup>11</sup> A. A. P. Suaide,<sup>30</sup> E. Sugarbaker,<sup>20</sup> C. Suire,<sup>13</sup> M. Šumbera,<sup>9</sup> T. J. M. Symons,<sup>15</sup> A. Szanto de Toledo,<sup>25</sup> P. Szarwas,<sup>28</sup> J. Takahashi,<sup>25</sup> A. H. Tang,<sup>14</sup> J. H. Thomas,<sup>15</sup> V. Tikhomirov,<sup>18</sup> T. A. Trainor,<sup>29</sup> S. Trentalange,<sup>6</sup> M. Tokarev,<sup>9</sup> M. B. Tonjes,<sup>17</sup> V. Trofimov,<sup>18</sup> O. Tsai,<sup>6</sup> K. Turner,<sup>2</sup> T. Ullrich,<sup>2</sup> D. G. Underwood,<sup>1</sup> G. Van Buren,<sup>2</sup> A. M. VanderMolen,<sup>17</sup> A. Vanyashin,<sup>15</sup> I. M. Vasilevski,<sup>10</sup> A. N. Vasiliev,<sup>22</sup> S. E. Vigdor,<sup>12</sup> S. A. Voloshin,<sup>30</sup> F. Wang,<sup>23</sup> H. Ward,<sup>27</sup> J. W. Watson,<sup>14</sup> R. Wells,<sup>20</sup> T. Wenaus,<sup>2</sup> G. D. Westfall,<sup>17</sup> C. Whitten, Jr.,<sup>6</sup> H. Wieman,<sup>15</sup> R. Willson,<sup>20</sup> S. W. Wissink,<sup>12</sup> R. Witt,<sup>14</sup> N. Xu,<sup>15</sup> Z. Xu,<sup>31</sup> A. E. Yakutin,<sup>22</sup> E. Yamamoto,<sup>6</sup> J. Yang,<sup>6</sup> P. Yepes,<sup>24</sup> A. Yokosawa,<sup>1</sup> V. I. Yurevich,<sup>9</sup> Y. V. Zanevski,<sup>9</sup> I. Zborovský,<sup>9</sup> H. Zhang,<sup>31</sup> W. M. Zhang,<sup>14</sup> R. Zoukarneev,<sup>10</sup> and A. N. Zubarev<sup>9</sup>

(STAR Collaboration)

<sup>1</sup>Argonne National Laboratory, Argonne, Illinois 60439<sup>2</sup>Brookhaven National Laboratory, Upton, New York 11973<sup>3</sup>University of Birmingham, Birmingham, United Kingdom<sup>4</sup>University of California, Berkeley, California 94720<sup>5</sup>University of California, Davis, California 95616<sup>6</sup>University of California, Los Angeles, California 90095<sup>7</sup>Carnegie Mellon University, Pittsburgh, Pennsylvania 15213<sup>8</sup>Creighton University, Omaha, Nebraska 68178<sup>9</sup>Laboratory for High Energy, JINR, Dubna, Russia<sup>10</sup>Particle Physics Laboratory, JINR, Dubna, Russia<sup>11</sup>University of Frankfurt, Frankfurt, Germany<sup>12</sup>Indiana University, Bloomington, Indiana 47408<sup>13</sup>Institut de Recherches Subatomiques, Strasbourg, France<sup>14</sup>Kent State University, Kent, Ohio 44242<sup>15</sup>Lawrence Berkeley National Laboratory, Berkeley, California 94720<sup>16</sup>Max-Planck-Institut für Physik, Munich, Germany<sup>17</sup>Michigan State University, East Lansing, Michigan 48824

<sup>18</sup>*Moscow Engineering Physics Institute, Moscow, Russia*<sup>19</sup>*City College of New York, New York, New York 10031*<sup>20</sup>*Ohio State University, Columbus, Ohio 43210*<sup>21</sup>*Pennsylvania State University, University Park, Pennsylvania 16802*<sup>22</sup>*Institute of High Energy Physics, Protvino, Russia*<sup>23</sup>*Purdue University, West Lafayette, Indiana 47907*<sup>24</sup>*Rice University, Houston, Texas 77251*<sup>25</sup>*Universidade de Sao Paulo, Sao Paulo, Brazil*<sup>26</sup>*SUBATECH, Nantes, France*<sup>27</sup>*University of Texas, Austin, Texas 78712*<sup>28</sup>*Warsaw University of Technology, Warsaw, Poland*<sup>29</sup>*University of Washington, Seattle, Washington 98195*<sup>30</sup>*Wayne State University, Detroit, Michigan 48201*<sup>31</sup>*Yale University, New Haven, Connecticut 06520*

(Received 17 August 2001; published 21 March 2002)

We present the first measurement of midrapidity vector meson  $\phi$  production in Au+Au collisions at RHIC ( $\sqrt{s_{NN}}=130$  GeV) from the STAR detector. For the 11% highest multiplicity collisions, the slope parameter from an exponential fit to the transverse mass distribution is  $T=379\pm 50(\text{stat})\pm 45(\text{syst})$  MeV, the yield  $dN/dy=5.73\pm 0.37(\text{stat})\pm 0.69(\text{syst})$  per event, and the ratio  $N_\phi/N_{h^-}$  is found to be  $0.021\pm 0.001(\text{stat})\pm 0.004(\text{syst})$ . The measured ratio  $N_\phi/N_{h^-}$  and  $T$  for the  $\phi$  meson at midrapidity do not change for the selected multiplicity bins.

DOI: 10.1103/PhysRevC.65.041901

PACS number(s): 25.75.Dw

The central topic of relativistic heavy ion physics is the study of quantum chromodynamics (QCD) in extreme conditions of high temperature and high energy density over large volumes [1]. Vector mesons may probe the dynamics of particles and chiral symmetry [2] in relativistic heavy ion collisions: their production mechanisms and subsequent dynamical evolution have been a topic of experimental investigation [4,3,5,6]. The  $\phi$  meson is of particular interest due to its  $s\bar{s}$  valence quark content, which may make the  $\phi$  sensitive to strangeness production from a possible early partonic phase [7–10].

In central Pb+Pb collisions at SPS (nucleon-nucleon center-of-mass energy  $\sqrt{s_{NN}}=17$  GeV), the slope parameter ( $T$ ) in an exponential fit to the transverse mass ( $m_t$ ) distribution at midrapidity ( $\propto e^{-m_t/T}$ ) follows a systematic trend as a function of hadron mass for pions, kaons, and protons [11]. This observation is indicative of a common expansion velocity developed in the final state for pions, kaons, and protons [12]. The slope parameters, however, measured for multi-strange hyperons  $\Xi$  and  $\Omega$  [13], and for  $J/\psi$  [14] show deviations from a linear mass dependence, suggesting that these particles do not interact as strongly in the final state at SPS energies [15]. Measurements of  $\phi$  meson production at the SPS were inconclusive [3,4]. Largely different values for the  $\phi$  slope parameter have been obtained from exponential fits to the measured  $m_t$  spectra in central Pb+Pb collisions when using the  $K^+K^-$  decay channel [3] and when using the  $\mu^+\mu^-$  decay channel [4] of the  $\phi$  meson. This difference, however, is not apparent in peripheral collisions [16,17]. Possible scenarios to explain the difference have been discussed in the literature [18,19].

In this Rapid Communication, we report the first measurement of midrapidity ( $|y|<0.5$ )  $\phi$  production in Au+Au col-

lisions at RHIC ( $\sqrt{s_{NN}}=130$  GeV) via the  $\phi\rightarrow K^+K^-$  decay channel (branching ratio = 0.491) using the Solenoidal Tracker at RHIC (STAR) detector [20]. Systematics of  $\phi$  production as a function of centrality at RHIC as well as its  $\sqrt{s_{NN}}$  dependence will be discussed.

The STAR detector consists of several detector subsystems in a large solenoidal analyzing magnet. For the data taken in the year 2000 and presented here, the experimental setup consisted of a time projection chamber (TPC) [21], a central trigger barrel (CTB), and two zero degree calorimeters (ZDC) located upstream along the beam axis. The TPC is a cylindrical drift chamber with multiwire proportional chamber readout. With its axis aligned along the beam direction, the TPC provided complete azimuthal coverage. Surrounding the TPC was the CTB, which measured energy deposition from charged particles. The ZDC measured beam-like neutrons from the fragmentation of colliding nuclei. The CTB was used in conjunction with the ZDC as the experimental trigger.

Data used in this analysis were taken with two different trigger conditions: a minimum-bias trigger requiring a coincidence between both ZDC's and a central trigger additionally requiring a high hit multiplicity in the CTB. The central trigger corresponded to approximately the top 15% of the measured cross section for Au+Au collisions. Data from both the minimum-bias trigger and central trigger were used for this analysis.

Reconstruction of the  $\phi$  was accomplished by calculating the invariant mass ( $m_{inv}$ ), transverse momentum ( $p_t$ ), and rapidity ( $y$ ) of all permutations of candidate  $K^+K^-$  pairs. The resulting  $m_{inv}$  distribution consisted of the  $\phi$  signal atop a large background that is predominantly combinatorial. The shape of the combinatorial background was calculated using the mixed-event technique [22,23].

For the centrality measurement, the raw total charged multiplicity distribution within a pseudorapidity window  $|\eta| \leq 0.75$  was divided into three bins corresponding to 85–26%, 26–11%, and the top 11% of the measured cross section for Au+Au collisions [24–26]. Events were selected with a primary vertex  $z$  position ( $z$ ) from the center of the TPC of  $|z| < 80$  cm. These events were further divided according to  $z$  in 16 bins, and event mixing was performed for events within each bin to construct background distributions with reduced acceptance-induced distortions in the mixed-event background. Consistent results were obtained when we constructed the background distribution using like-sign pairs from the same event.

Particle identification (PID) was achieved by correlating the ionization energy loss ( $dE/dx$ ) of charged particles in the TPC gas with their measured momentum [26,27]. By truncating the largest 30%  $dE/dx$  values along the track a sample was selected to calculate the mean  $\langle dE/dx \rangle$ . For the highest multiplicity events, the average  $\langle dE/dx \rangle$  resolution was found to be about 11%. The measured  $\langle dE/dx \rangle$  is reasonably described by the Bethe-Bloch function smeared with a resolution of width  $\sigma$ . Tracks within  $2\sigma$  of the kaon Bethe-Bloch curve were selected for this analysis.

To obtain the  $\phi$  spectra, same event and mixed event distributions were accumulated and background subtraction was done in each  $(m_t, y)$  bin. The mixed event background  $m_{inv}$  distribution was normalized to the same event  $m_{inv}$  distribution in the region above the  $\phi$  mass ( $1.04 < m_{inv} < 1.2$  GeV/ $c^2$ ). A small, smooth residual background can remain near the  $\phi$  peak in the subtracted mass distribution, because the mixed event sample does not properly account for the production of background pairs (kaons and/or pions from PID leak-through) that are correlated, either by Coulomb or other interactions or by such instrumental effects as track merging [27]. The yield in each bin was then determined by fitting the background subtracted  $m_{inv}$  distribution to a Breit-Wigner function plus a linear background in a limited mass range (Fig. 1). The signal-to-background ratios are approximately 1/30 and 1/120 in Figs. 1(a) and 1(b), respectively.

Figure 1(b) shows the  $m_{inv}$  distribution in a relatively high  $p_t$  bin which has a residual background. The shape of the residual background is not well constrained by the statistically limited data in this particular bin, but the linear assumption worked well for all momentum bins. The widths of the fits to the invariant mass distribution are consistent with the natural width of the  $\phi$  convoluted with the resolution of the TPC. The uncertainties in the extracted  $\phi$  yields are dominated by the statistical errors derived from the fitting procedure, which include the statistical uncertainty from the mixed event background subtraction. The resulting raw  $\phi$  yield for each  $m_t$ ,  $y$ , and multiplicity bin was then corrected for tracking efficiency and acceptance using Monte Carlo simulations of physics processes and detector response. The overall correction factor for efficiency and acceptance depended on the  $p_t$  of the  $\phi$ , ranging from  $\sim 10\%$  at  $p_t = 0.46$  GeV/ $c$  up to  $\sim 40\%$  at  $p_t = 1.4$  GeV/ $c$ . The PID efficiency correction for the  $\phi$  was calculated as the square of the single kaon PID efficiency and included the multiplic-

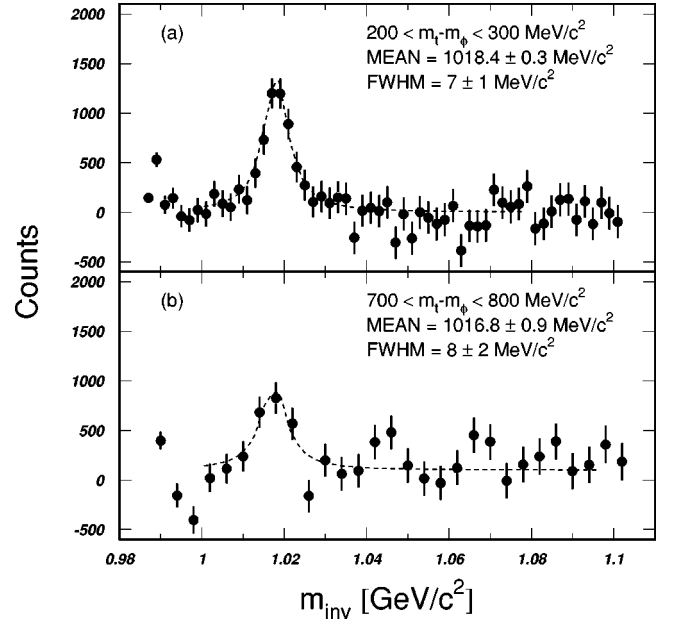


FIG. 1. Invariant mass distributions for candidate  $K^+K^-$  pairs in two  $m_t - m_\phi$  bins after background subtraction for the 11% most central collisions. Bins in panel (a) are 2 MeV/ $c^2$  wide while the bins in panel (b) are 4 MeV/ $c^2$  wide. The mass and widths of the mass distributions are consistent with the natural mass and width of the  $\phi$  convoluted with the resolution of the TPC. Error bars shown are statistical only.

ity dependence of the  $dE/dx$  resolution. The corrected  $\phi$  invariant yields for three event multiplicity bins are shown in Fig. 2. All results presented here are for reconstructed  $\phi$  mesons within one unit of rapidity centered around  $y=0$  ( $|y| < 0.5$ ) and  $0.46 < p_t < 1.74$  GeV/ $c$ . In the region where the pion band crosses the kaon band in  $dE/dx$  [26], corresponding to the kaon  $p_t \approx 0.8$  GeV/ $c$  the signal to background ratio degrades. This leads to the larger statistical error bars in the most central bin and prevented the extraction of the  $\phi$  yields in this region for the two lower multiplicity bins. The spectra were fit to an exponential

$$\frac{1}{2\pi m_t} \frac{d^2N}{dm_t dy} = \frac{dN/dy}{2\pi T(m_\phi + T)} e^{-(m_t - m_\phi)/T}, \quad (1)$$

with the slope parameter  $T$  and yield  $dN/dy$  set as free parameters. The obtained results are listed in Table I. The fraction of  $\phi$  mesons in the measured  $p_t$  region assuming an exponential distribution is  $\sim 70\%$ . Also listed is the midrapidity ratio of the  $\phi$  yield to the negative hadron ( $h^-$ ) yield [28] for three multiplicity bins.

The major systematic uncertainties for this analysis include contributions from PID efficiency and tracking efficiency. The systematic error based on different background fits is significantly smaller than the statistical error in all  $p_t$  bins. By varying PID and track quality requirements, we estimate a systematic uncertainty of  $\pm 12\%$  for  $T$ . The total systematic error on  $dN/dy$  is  $\pm 12\%$  which includes an additional 6% uncertainty (added in quadrature) due to uncertainties in TPC performance. Systematic errors for the ratios

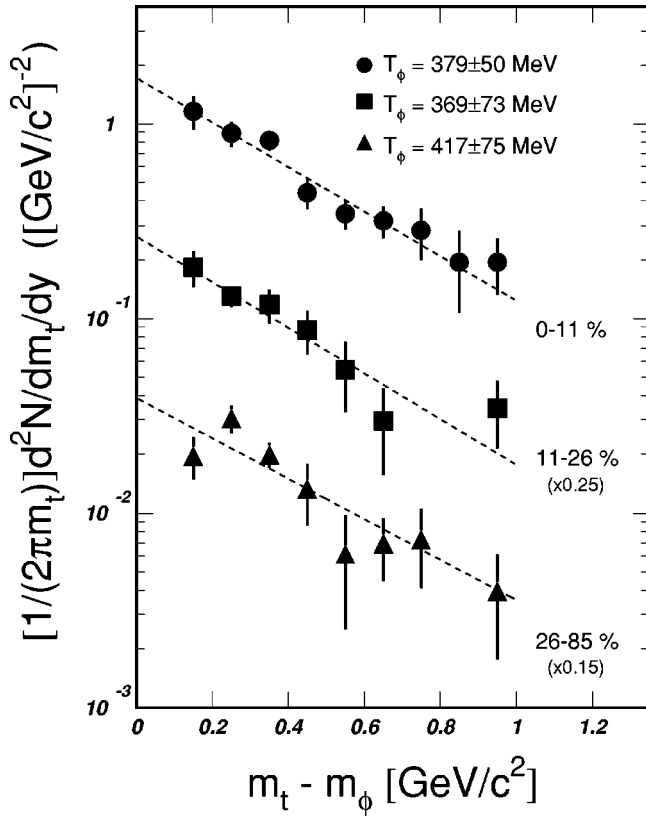


FIG. 2. Transverse mass distributions of  $\phi$  from Au+Au collision at  $\sqrt{s_{NN}} = 130$  GeV for three multiplicity bins. Dashed lines are exponential fits to the data. For clarity, data points from the 11–26% and 26–85% multiplicity bins are scaled by 0.25 and 0.15, respectively. Error bars shown are statistical only.

also include uncertainties from the  $h^-$  yields. The full range of the systematic uncertainty for  $N_\phi/N_{h^-} \pm 22\%$ .

Figure 3 shows a comparison of our results for the  $\phi$  slope parameter to previous measurements at lower collision energies. Filled symbols represent results extracted from the most central heavy ion collisions (10% for [3] and 23% for [6]) and the open symbols represent the results from  $p+p$  collisions [3,29]. For heavy ion collisions, there is an increase in  $T$  from the AGS ( $\sqrt{s_{NN}} \approx 5$  GeV) to SPS ( $\sqrt{s_{NN}} \approx 17$  GeV) to RHIC ( $\sqrt{s_{NN}} = 130$  GeV). Slope parameters from  $p+p$  collisions show no significant dependence on collision energy up to  $\sqrt{s} = 63$  GeV.

Since the  $\phi$  and antiproton have similar masses and very different scattering cross sections [8], comparison of the spectral shapes would shed light on collision dynamics. In

TABLE I. Midrapidity  $\phi$  slope parameters  $T$ , extrapolated yield  $dN/dy$ , and the ratio  $N_\phi/N_{h^-}$  for three multiplicity bins. Errors shown are statistical only.

Event multiplicity	0–11 %	11–26 %	26–85 %
$T$ (MeV)	$379 \pm 50$	$369 \pm 73$	$417 \pm 75$
$dN/dy$	$5.73 \pm 0.37$	$3.33 \pm 0.38$	$0.98 \pm 0.12$
$N_\phi/N_{h^-}$	$0.021 \pm 0.001$	$0.019 \pm 0.002$	$0.019 \pm 0.002$

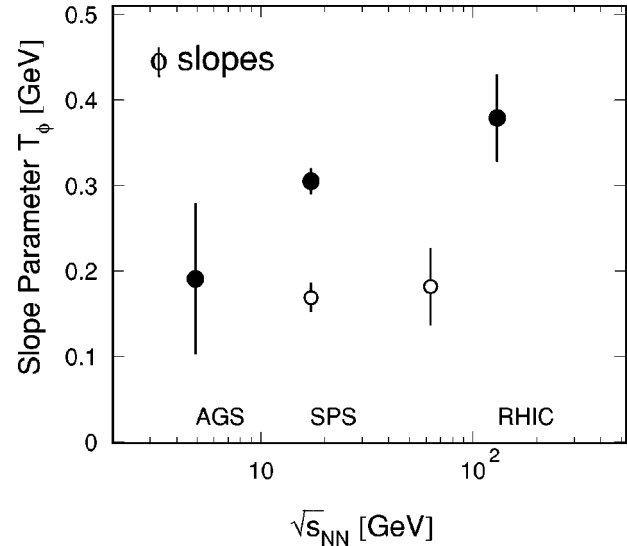


FIG. 3.  $\sqrt{s_{NN}}$  dependence of the midrapidity  $\phi$  slope parameter. The data points are from the  $\phi \rightarrow K^+K^-$  decay channel. Filled symbols represent the results extracted from the highest multiplicity heavy ion collisions and the open symbols represent the results from  $p+p$  collisions. Error bars shown are statistical errors only.

the highest multiplicity Au+Au collisions at RHIC, the  $\phi$  slope parameter is  $379 \pm 50$  (stat)  $\pm 45$  (syst) and there is no dependence on event multiplicity (Table I) within our statistical uncertainty. The antiproton slope parameter using the same fit function, however, measured in the  $p_t$  range  $0.25 < p_t < 1$  GeV/c and without correction for feed-down from antihyperons, is found to be over 150 MeV higher than the  $\phi$  meson slope measured in  $0.5 < p_t < 1.7$  GeV/c [30]. Note

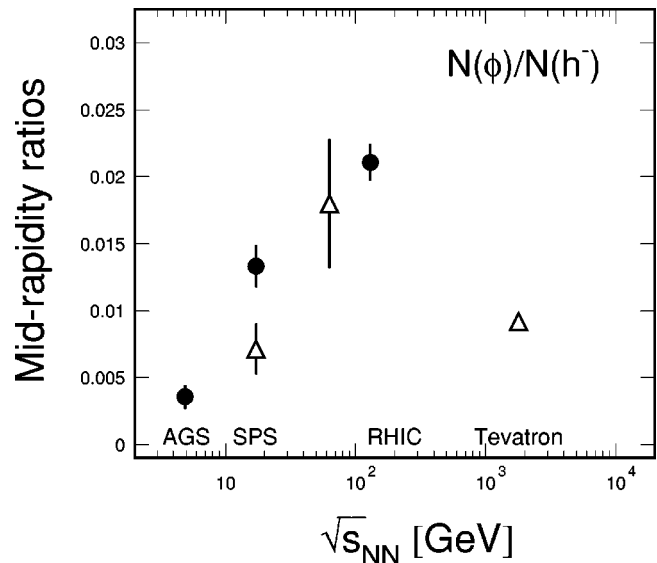


FIG. 4.  $\sqrt{s_{NN}}$  dependence of the midrapidity  $N_\phi/N_{h^-}$  ratio. Results were extracted from the  $\phi \rightarrow K^+K^-$  decay channel. Filled symbols represent the results extracted from the highest multiplicity heavy ion collisions and the open symbols represent the results from  $p+p$  (17 and 63 GeV points) and  $p+\bar{p}$  (1800 GeV) collisions. Error bars shown are statistical errors only.

that if a strong collective flow develops in the system, the measured slope parameter should depend strongly on the fitting range. Measurements of the  $\phi$  and antiproton over a much broader range of  $p_t$  will yield a more definitive conclusion on the dynamics of these particles. The energy dependence of the midrapidity  $N_\phi/N_{h^-}$  is shown in Fig. 4. In heavy ion collisions,  $N_\phi/N_{h^-}$  increases with collision energy indicating that  $\phi$  production increases faster than  $h^-$  production up to  $\sqrt{s_{NN}}=130$  GeV. Although there seems to be a significant increase in  $N_\phi/N_{h^-}$  ratio from  $p+p$  collisions between 17 and 63 GeV [3,29], the statistical uncertainty in the 63 GeV point is too large to determine the energy dependence. Note that the ratio at Tevatron energies ( $p+\bar{p}$  at  $\sqrt{s}=1800$  GeV) was found to be about 0.01 [31].

In summary, using the STAR detector we have measured midrapidity  $\phi$  production from Au+Au collisions at  $\sqrt{s_{NN}}=130$  GeV. In the most central collisions, the  $\phi$  slope parameter,  $T=379\pm 50$  (stat) $\pm 45$  (syst) MeV, is lower than that of antiprotons in the measured  $p_t$  region. Within statis-

tical uncertainty, there is no variation in  $\phi$  slope parameters and the ratio  $N_\phi/N_{h^-}$  for the selected multiplicity bins. The  $\phi$  slope parameter and the ratio  $N_\phi/N_{h^-}$  increase from  $\sqrt{s_{NN}}\approx 5$  to 130 GeV.

We wish to thank the RHIC Operations Group and the RHIC Computing Facility at Brookhaven National Laboratory, and the National Energy Research Scientific Computing Center at Lawrence Berkeley National Laboratory for their support. This work was supported by the Division of Nuclear Physics and the Division of High Energy Physics of the Office of Science of the U. S. Department of Energy, the United States National Science Foundation, the Bundesministerium für Bildung und Forschung of Germany, the Institut National de la Physique Nucleaire et de la Physique des Particules of France, the United Kingdom Engineering and Physical Sciences Research Council, Fundacao de Amparo a Pesquisa do Estado de Sao Paulo, Brazil, and the Russian Ministry of Science and Technology.

- 
- [1] F. Wilczek, Phys. Today, **53**, 22 (2000).  
 [2] T. Hatsuda and T. Kunihiro, Phys. Rep. **247**, 221 (1994).  
 [3] NA49 Collaboration, S.V. Afanasiev *et al.*, Phys. Lett. B **491**, 59 (2000).  
 [4] NA50 Collaboration, N. Willis *et al.*, Nucl. Phys. **A661**, 534c (1999).  
 [5] E802 Collaboration, Y. Akiba *et al.*, Phys. Rev. Lett. **76**, 2021 (1996).  
 [6] E917 Collaboration, R.K. Seto and H. Xiang, Nucl. Phys. **A661**, 506c (1999).  
 [7] J. Rafelski and B. Müller, Phys. Rev. Lett. **48**, 1066 (1982).  
 [8] A. Shor, Phys. Rev. Lett. **54**, 1122 (1985).  
 [9] P. Koch, B. Müller, and J. Rafelski, Phys. Rep. **142**, 167 (1986).  
 [10] S.A. Bass *et al.*, Nucl. Phys. **A661**, 205 (1999).  
 [11] NA44 Collaboration, I. Bearden *et al.*, Phys. Rev. Lett. **78**, 2080 (1997).  
 [12] U. Heinz, Nucl. Phys. **A610**, 264c (1996).  
 [13] WA97 Collaboration, E. Andersen *et al.*, Phys. Lett. B **433**, 209 (1998).  
 [14] NA50 Collaboration, M.C. Abreu *et al.*, Phys. Lett. B **499**, 85 (2001).  
 [15] H. van Hecke, H. Sorge, and N. Xu, Phys. Rev. Lett. **81**, 5764 (1998).  
 [16] NA49 Collaboration, V. Friese *et al.*, Quark Matter, 2001.  
 [17] NA50 Collaboration, C. Quintans *et al.*, J. Phys. G **27**, 405c (2001).  
 [18] S. Johnson, B. Jacak, and A. Drees, Eur. Phys. J. C **18**, 645 (2001).  
 [19] S. Soff *et al.*, J. Phys. G **27**, 449c (2001).  
 [20] STAR Collaboration, K.H. Ackermann *et al.*, Nucl. Phys. **A661**, 681c (1999).  
 [21] H. Wieman *et al.*, IEEE Trans. Nucl. Sci. **44**, 671 (1997).  
 [22] D. L'Hote, Nucl. Instrum. Methods Phys. Res. A **337**, 544 (1994).  
 [23] D. Drijard, H.G. Fischer, and T. Nakada, Nucl. Instrum. Methods Phys. Res. A **225**, 367 (1984).  
 [24] STAR Collaboration, K.H. Ackermann *et al.*, Phys. Rev. Lett. **86**, 402 (2001).  
 [25] The measured cross section is approximately 90% of the total inelastic Au+Au cross section. Our centrality bins correspond to approximately 77–23%, 23–10%, and top 10% of the inelastic Au+Au cross section.  
 [26] STAR Collaboration, J. Harris *et al.*, Nucl. Phys. **A698**, 64c (2002).  
 [27] E. Yamamoto, Ph.D. thesis, University of California–Los Angeles, 2001.  
 [28] C. Adler *et al.*, Phys. Rev. Lett. **87**, 112303 (2001).  
 [29] AFS Collaboration, T. Åkesson *et al.*, Nucl. Phys. **B203**, 27 (1982).  
 [30] C. Adler *et al.*, STAR Collaboration, Phys. Rev. Lett. (submitted).  
 [31] E735 Collaboration, T. Alexopoulos *et al.*, Phys. Rev. D **48**, 984 (1993); E735 Collaboration, T. Alexopoulos *et al.*, Z. Phys. C **67**, 411 (1995).